

Supporting Information

Oxygen defect regulation and photocatalytic-peroxymonosulfate activation of Co(II)/BiPO_{4-x} composites synergistically promoting medical waste degradation

Jiaying Zhang ^{1ac}, Fan Fan ^{1ab}, Wei Zhu ^d, Wenqing Yao ^b, Fupeng Zhao ^a, Zhuang Yang ^a, Cong Wang ^a and Yajun Wang ^{*a}

^a State Key Laboratory of Heavy Oil Processing, College of New Energy and Materials, China University of Petroleum, Beijing, Beijing 102249, PR China

^b Department of Chemistry, Beijing Key Laboratory for Analytical Methods and Instrumentation, Tsinghua university, Beijing 100084, PR China

^c Organic Chemical Plant of Sinopec Beijing Yanshan Company, Beijing 102500

^d College of Environmental and Chemical Engineering, Xi'an Polytechnic University, Xi'an 710048, PR China

¹ J. Zhang and F. Fan contributed equally to this work.

*Corresponding Author: wangyajun@cup.edu.cn

1. Experimental Detail

1.1. Characterization of materials

X-ray diffraction (XRD) patterns were obtained by conducting powder XRD using a Bruker D8-advance X-ray diffractometer at 40 kV and 40 mA with Cu-K α ($\lambda = 1.5406 \text{ \AA}$) radiation. Fourier transform infrared spectroscopy (FT-IR) was measured on a Pekin-Elmer 2000 infrared spectrometer. The UV-vis diffuse reflectance spectroscopy (DRS) was recorded by a Hitachi U-3010 UV-vis spectrophotometer using BaSO₄ as the reference sample. The morphologies of the as-prepared samples were investigated by an FEI Tecnai F20 transmission electron microscope operated at an accelerating voltage of 150 kV and a Hitachi SU-8010 field emission gun scanning electron microscope. The chemical states of the as-prepared samples were examined through X-ray photoelectron spectroscopy (XPS) (Thermo Fisher K-Alpha

instrument). XPS was carried out on a PHI Quantera ULVAC XPS (USA) system. The binding energies were normalized by adventitious carbon with a binding energy of 284.6 eV. The Perkin-Elmer LS55 fluorescence spectrometer (PL) was used, with a wavelength range of 200-800 nm and an accuracy of ± 1.2 nm. The excitation wavelength was 254 nm. The photocurrents and electrochemical impedance spectra (EIS) were measured on an electrochemical system (CHI 660D, China). A standard three-electrode cell with a working electrode (as-prepared photocatalyst), a platinum wire as counter electrode, and a standard calomel electrode as reference electrode were used in the photoelectric studies. 0.1M Na₂SO₄ was used as the electrolyte solution. The ultraviolet light source was a 17 W low-pressure mercury lamp. Potentials are given concerning the SCE. The photoresponses of the photocatalysts as light on and off were measured at 0.0 V. The test frequency range of EIS is 0.05-10⁵ Hz, and the amplitude is 5 mV. Electron paramagnetic resonance spectrometer (EPR) JEOL ES-ED3X model was used. The defect test was performed at a low temperature of 77 K to amplify the detection signal, and the g value was calculated by the manganese standard. Agilent 7890B-5977A gas chromatograph-mass spectrometer was used. The chromatographic column was Agilent DB-FFAP 30 mm \times 0.25 mm \times 0.25 μ m. The EI bombardment energy was 70 eV. The carrier gas was helium. The column temperature was increased to 280 °C at a heating rate of 15 °C/min. The inlet temperature was 260 °C and the ion source temperature was 230 °C.

1.2. Pretreatment and preparation of PET plastics

1 g of PET particles were placed in an autoclave with 50 mL of deionized water and then transferred to a 100 mL stainless steel autoclave lined with polytetrafluoroethylene. The mixture was then heated to 180°C and maintained at that temperature for 12 hours. Washed three times in deionized water and ethanol, dried at 60 °C, and marked it PET-12 and set aside.

1.3. Catalytic degradation evaluation

To evaluate the degradation activity, the multi-channel photochemical reactor of Beijing Porphyry PCX-50C Discover (operated at 20°C) was utilized. In this experiment, a certain amount of catalyst was dispersed in a 50 mL tetracycline hydrochloride solution (with an initial concentration of 50 ppm), and the resulting suspension was subjected to magnetic stirring for 120 minutes under dark conditions to achieve adsorption equilibrium. After equilibrium, a

certain concentration of PMS was added separately to the reaction flask, and then the light was immediately turned on for tetracycline hydrochloride degradation. Samples were taken at predetermined time intervals and then immediately added to centrifuge tubes containing 1 mL of methanol to burst the residual active species. The mixture was first separated by centrifugation, the supernatant was taken and the absorbance was detected sequentially at 358 nm using a New Century T6 ultraviolet-visible spectrophotometer, and the relative percent change was obtained by comparing the original solution. Control experiments were carried out without the addition of catalyst and PMS, and the operation procedure was the same as above.

In addition, the degradation activity of PET plastic was also evaluated. 25 mg of catalyst, 25mg of PET plastic after 12h of hydrothermal treatment, and 15.3mg PMS put into the reactor, add 50 ml of deionized water, stirred evenly, turn on the xenon lamp for lighting 6 h (operated at 20°C). After the reaction, the solid product was then filtered with a pre-weighed 0.1µm organic system filter head. Before weighing, the filter head was dried until the mass does not change. Furthermore, blank experiment and comparison experiments (with or without PMS, light and dark, with or without catalyst) were conducted. The degradation efficiency was calculated using the following formula (1):

$$\text{weight loss (\%)} = \frac{W_t - W_0}{W_0} \times 100\% \quad (1)$$

Where W_t is the weight of the remaining PET after the oxidation reaction, and W_0 is the preliminary weight of PET.

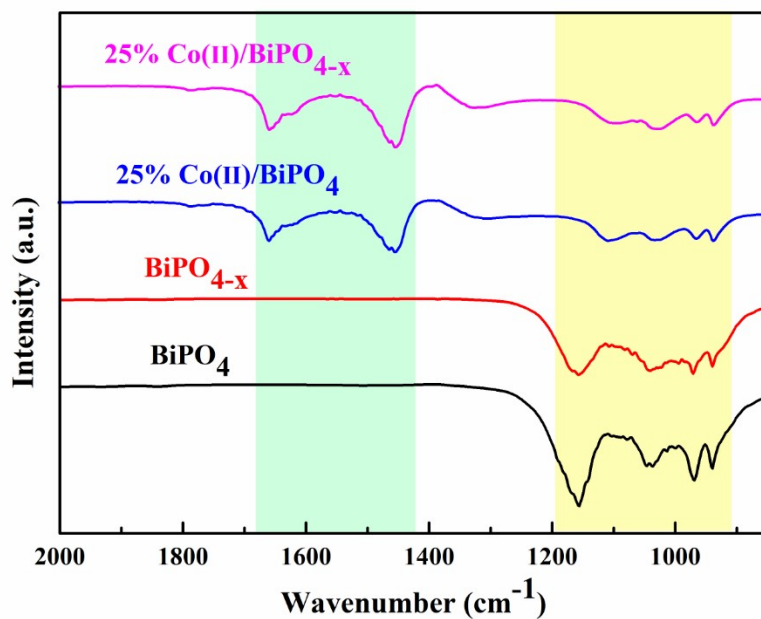


Fig. S1. FT-IR spectra of BiPO_4 , BiPO_{4-x} , $25\%\text{Co(II)/BiPO}_4$ and $25\%\text{Co(II)/BiPO}_{4-x}$.

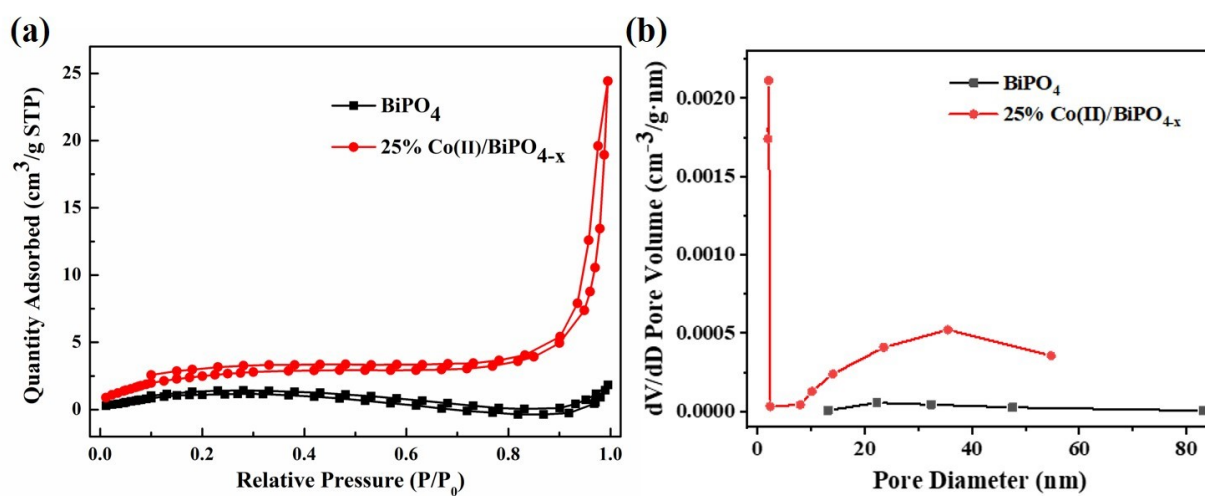


Fig. S2. (a) N_2 adsorption-desorption isotherms of BiPO_4 and $25\%\text{Co(II)/BiPO}_{4-x}$; (b) Pore size distribution profiles of BiPO_4 and $25\%\text{Co(II)/BiPO}_{4-x}$.

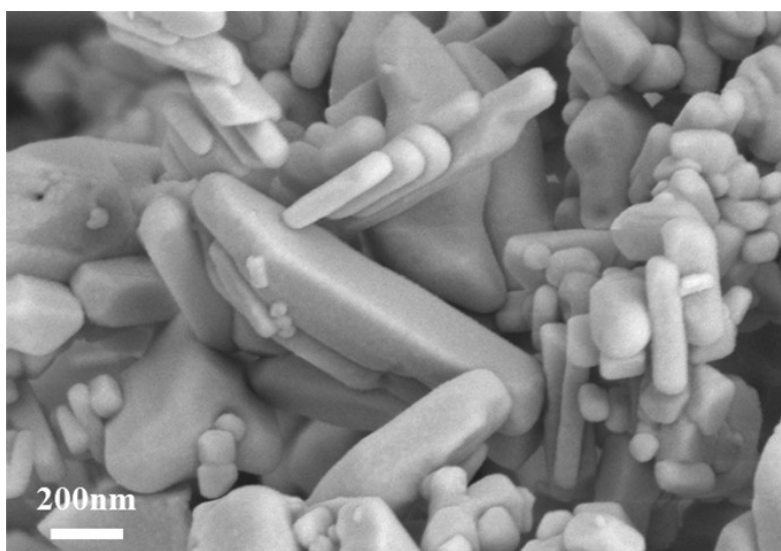


Fig. S3. SEM images of 25%Co(II)/BiPO₄.

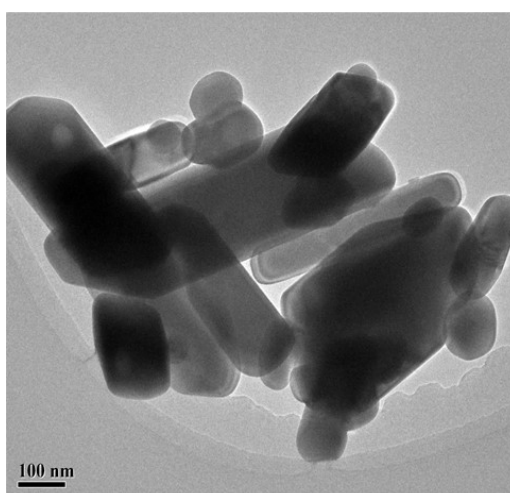


Fig. S4. TEM images of BiPO_{4-x}.

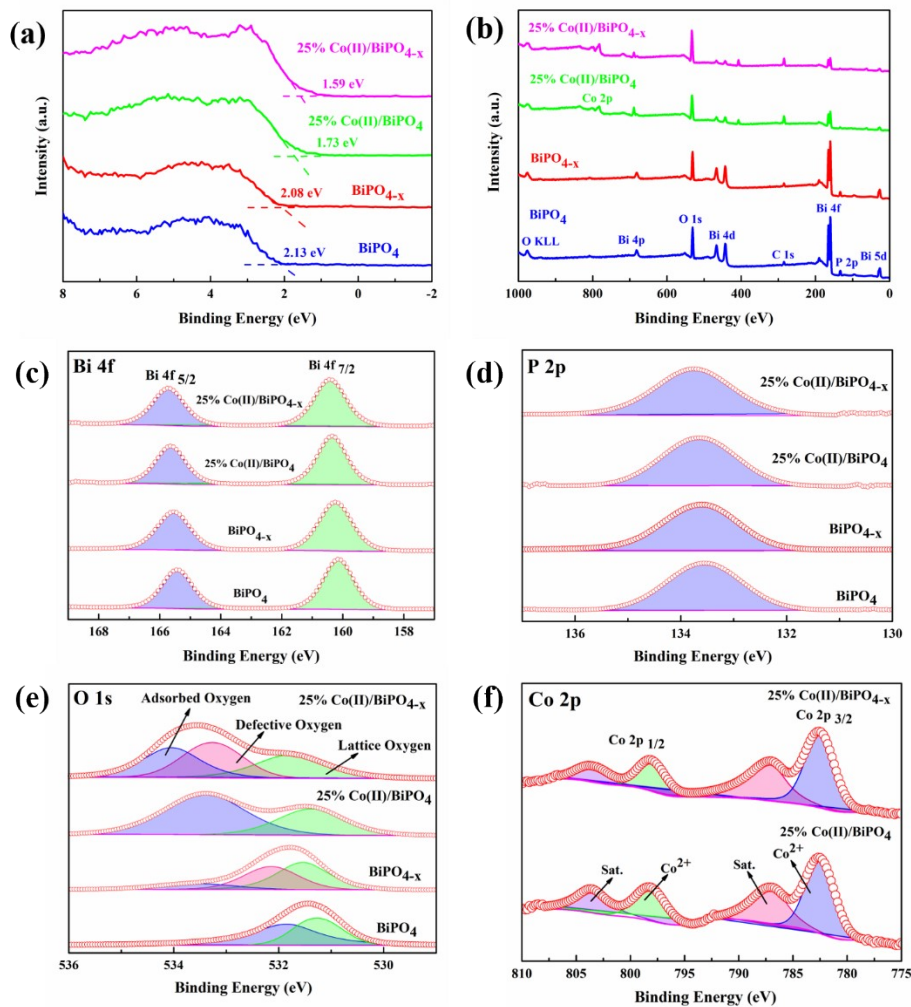


Fig. S5. The valence band spectra (a) and full spectra (b) of BiPO_4 , BiPO_{4-x} , $25\%\text{Co(II)/BiPO}_4$ and $25\%\text{Co(II)/BiPO}_{4-x}$; XPS spectra of BiPO_4 , BiPO_{4-x} , $25\%\text{Co(II)/BiPO}_4$ and $25\%\text{Co(II)/BiPO}_{4-x}$: (c) Bi 4f, (d) P 2p, (e) O 1s, (f) Co 2p.

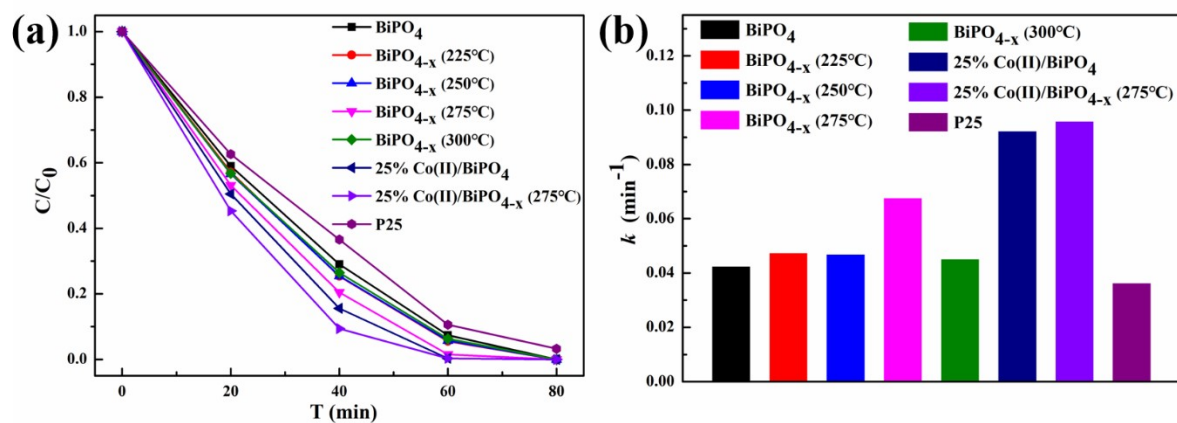


Fig. S6. (a) The TCH degradation curves; (b) reaction rate constant k of BiPO_4 , BiPO_{4-x} , $25\%\text{Co(II)/BiPO}_4$, $25\%\text{Co(II)/BiPO}_{4-x}$ and P25 in photocatalytic process ($\lambda=254\text{ nm}$)

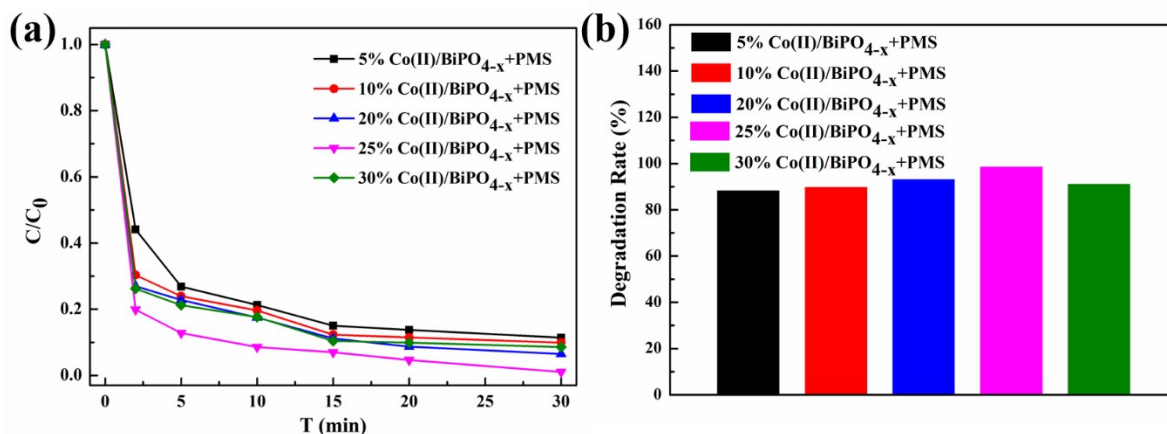


Fig. S7. (a) Effect of Co(II) contents on the TCH degradation in 25%Co(II)/BiPO_{4-x}/PMS/UV system; (b) Degradation rate of TCH in x%Co(II)/BiPO_{4-x} system

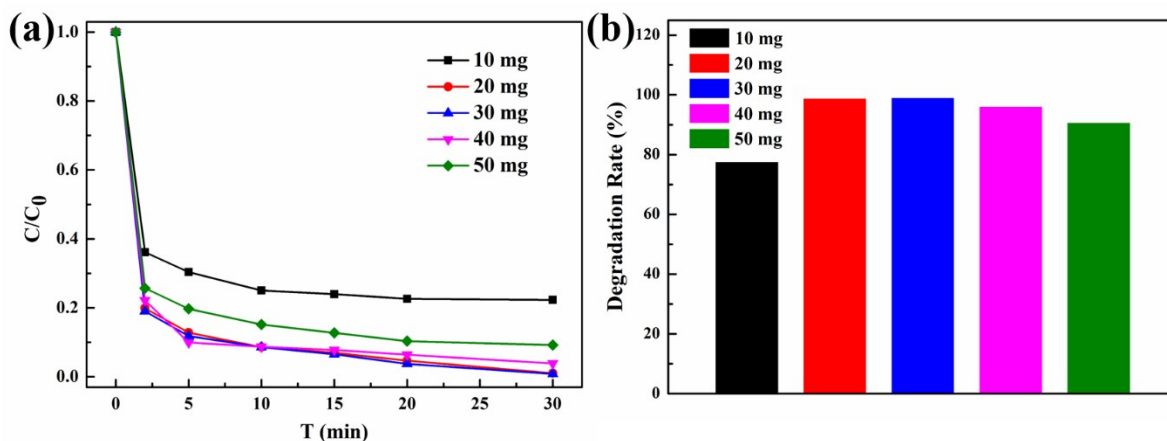


Fig. S8. (a) Effect of catalyst dosage on the TCH degradation in 25%Co(II)/BiPO_{4-x}/PMS/UV system; (b) Degradation rate of TCH under different catalyst dosages

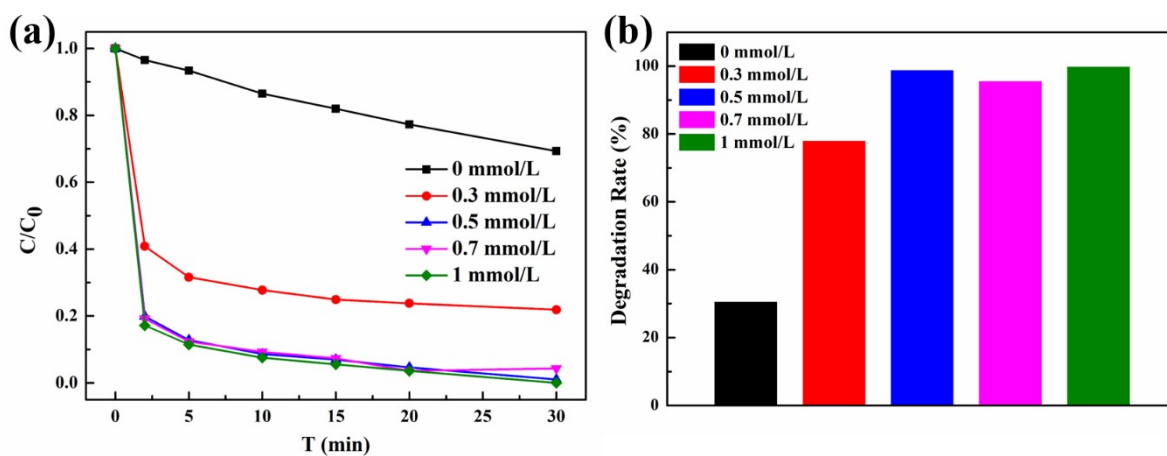


Fig. S9. (a) Effect of PMS dosage on the TCH degradation in 25%Co(II)/BiPO_{4-x}/PMS/UV system; (b) Degradation rate of TCH at different persulfate concentrations

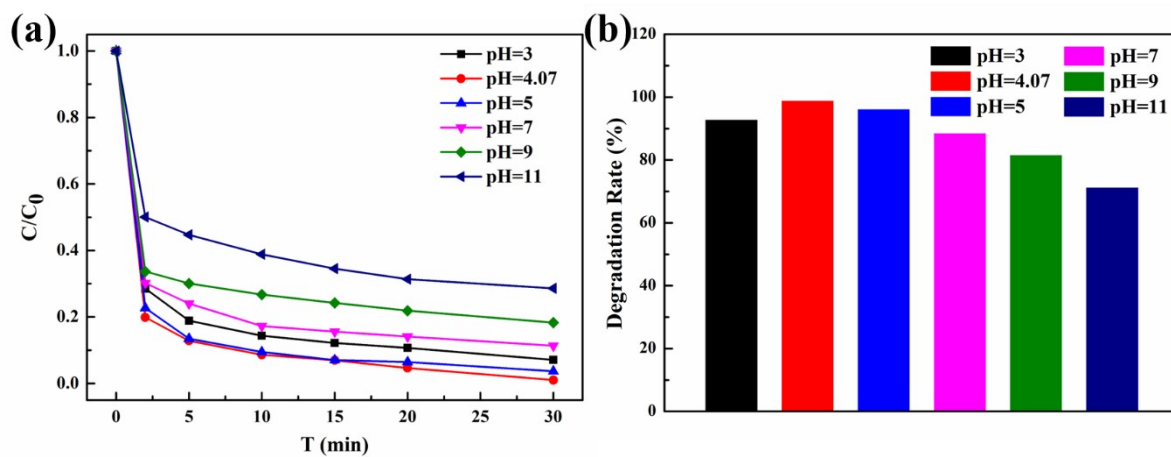


Fig. S10. (a) Effect of initial pH value on the TCH degradation in 25%Co(II)/BiPO₄_x/PMS/UV system; (b) Degradation rate of TCH at different pH values

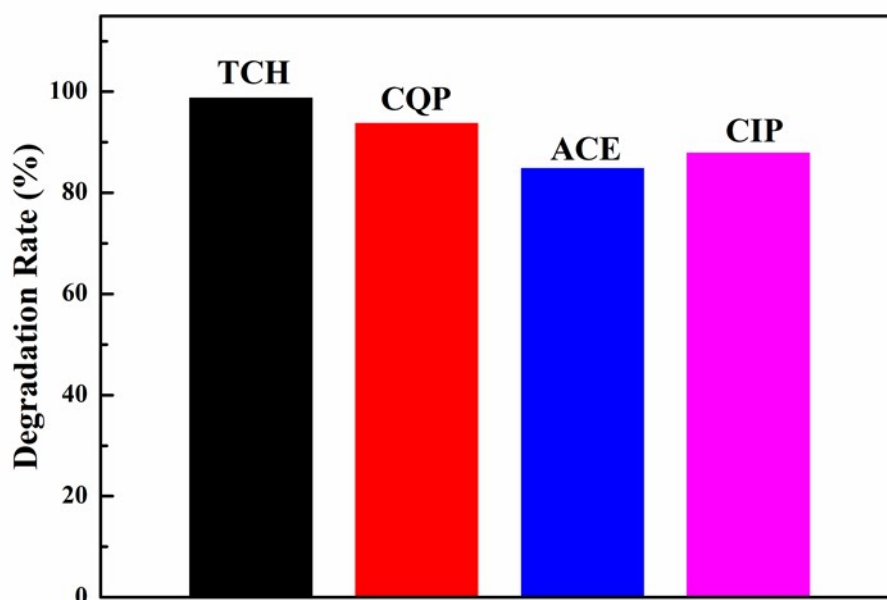


Fig. S11. Degradation rate of TCH under different pollutants

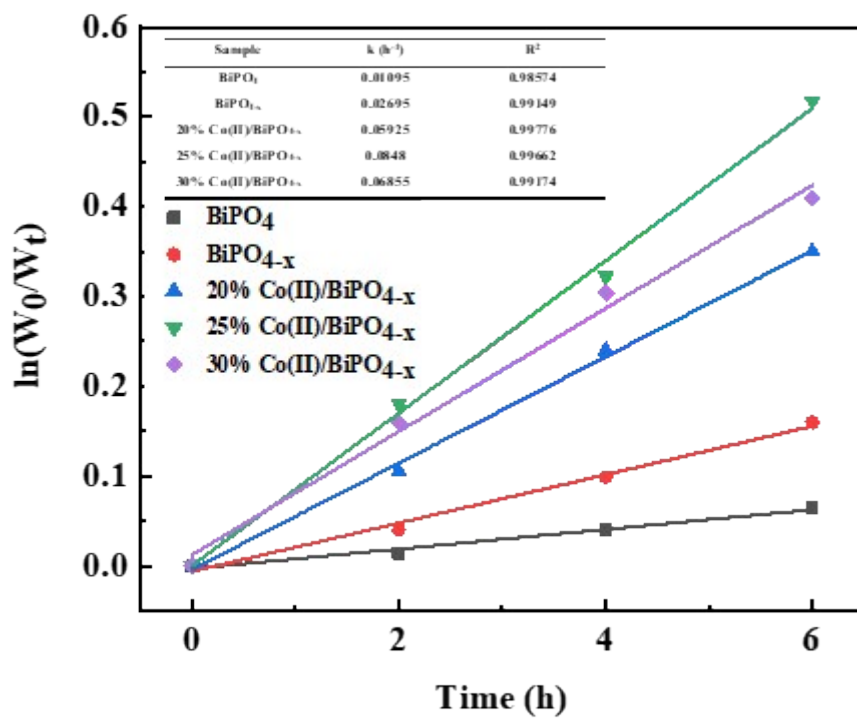


Fig. S12. The pseudo-first-order kinetic fitting curve of different photocatalysts

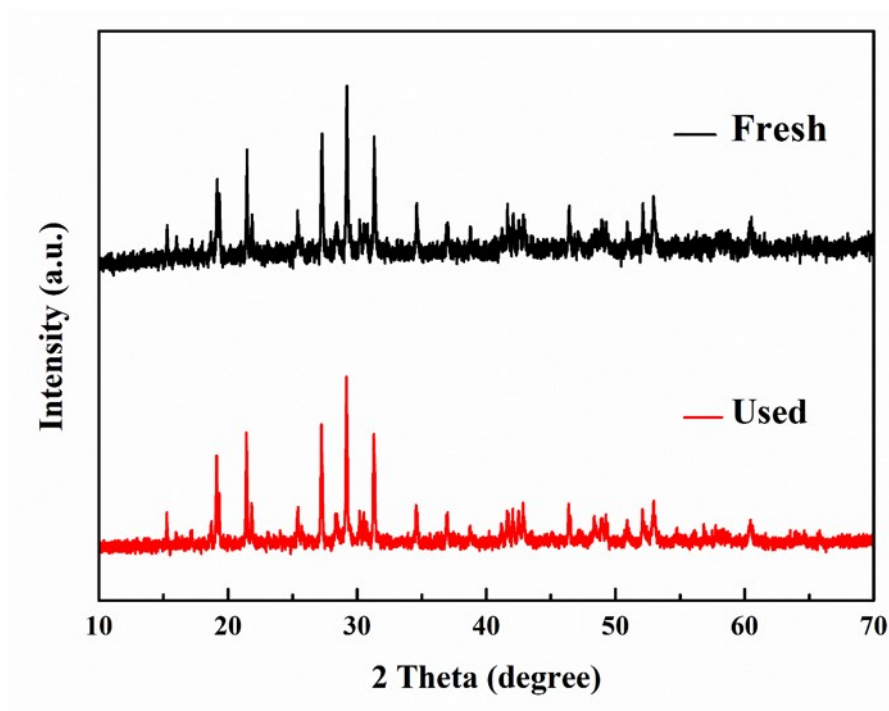


Fig. S13. XRD patterns of 25%Co(II)/BiPO_{4-x} before and after reaction

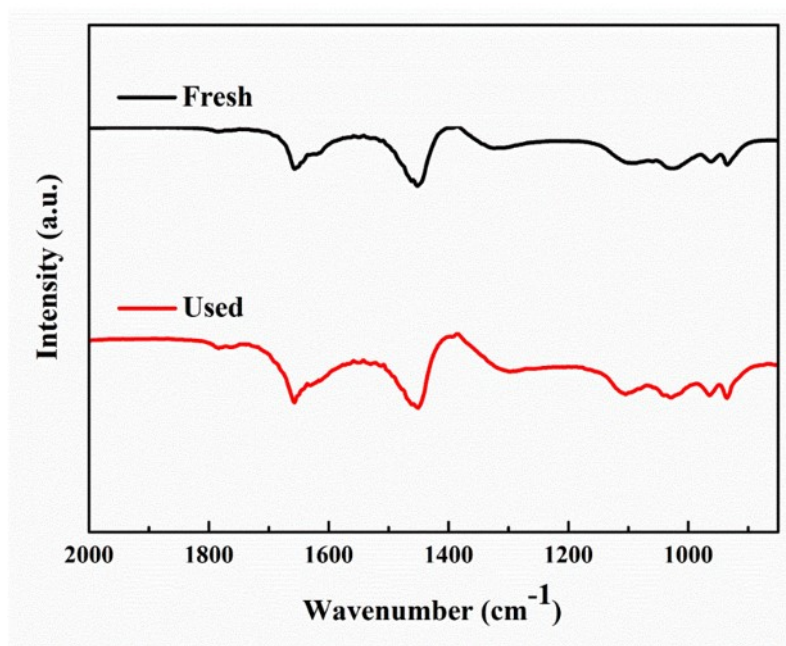


Fig. S14. FT-IR spectra of 25%Co(II)/BiPO_{4-x} before and after reaction

Table. S1. Specific surface area of BiPO₄ and 25%Co(II)/BiPO_{4-x}.

Catalysts	Surface Area (m ² /g)
BiPO ₄	5.4
25%Co(II)/BiPO _{4-x}	10.4

Table. S2. Energy band structure analysis of as-prepared x%Co(II)/BiPO_{4-x}.

Catalysts	band gap (eV)	CB (eV)	VB (eV)
BiPO ₄	4.27	-2.14	2.13
BiPO _{4-x}	4.20	-2.12	2.08
25%Co(II)/BiPO ₄	3.31	-1.58	1.73
25%Co(II)/BiPO _{4-x}	3.12	-1.53	1.59

Table. S3. Co content analysis of as-prepared x%Co(II)/BiPO_{4-x}.

Catalysts	content (wt%)
20%Co/BiPO _{4-x}	15.5
25%Co/BiPO ₄	19.9
25%Co(II)/BiPO _{4-x}	20.4
30%Co(II)/BiPO _{4-x}	23.5